Chinese Chemical Letters 37 (2026) 112033

Contents lists available at ScienceDirect

Chinese Chemical Letters

journal homepage: www.elsevier.com/locate/cclet

Anomeric configuration controls reductive amination efficiency: Structural and electronic insights into protein-monosaccharide conjugation

Jiaxu Zhang[a,b], Xianran He[a], Gilles Clodic[a], Leyu Tang[a], Jinge Cao[a], Yupeng Fu[a], Matthieu Sollogoub[a], Yongmin Zhang[a,b,c,*]

[a] Institut Parisien de Chimie Moléculaire, CNRS UMR8232, Sorbonne Université, 4 Place Jussieu, Paris 75005, France
[b] Translational Research Institute for Dermatology and Cosmetics, School of Biomedical and Pharmaceutical Sciences, Guangdong University of Technology, Guangzhou 510006, China
[c] Fuyang Institute & School of Pharmaceutical Sciences, Zhejiang Chinese Medical University, Hangzhou 310061, China

ARTICLE INFO

Article history:
Received 23 July 2025
Revised 14 October 2025
Accepted 29 October 2025
Available online 29 October 2025

Keywords:
Reductive amination
Glycoconjugation
Neoglycoprotein
Stereochemistry
Glycosidic functionalization

ABSTRACT

Reductive amination between glycolaldehyde derivatives and lysine residues is a widely used strategy for constructing neoglycoproteins in biomedical applications. Here, α- and β-glycolaldehyde glycosides of five biologically relevant monosaccharides (Glc, Gal, Man, GlcNAc, GalNAc) were synthesized and conjugated to protein at a fixed sugar-to-protein ratio. Continuous kinetic monitoring revealed that anomeric configuration markedly influences both reaction rates and final sugar loading: α-Man > β-Man; β-Gal/GalNAc > their α-counterparts; Glc and GlcNAc showed no significant anomeric preferences. NMR analysis identified cyclic intermediates that reduce the effective concentration of reactive aldehyde, while DFT calculations provided complementary insight into anomer-specific electrophilic character. These findings offer a mechanistic rationale for selecting anomeric configuration in glycoconjugate design.

© 2026 Published by Elsevier B.V. on behalf of Chinese Chemical Society and Institute of Materia Medica, Chinese Academy of Medical Sciences.

Carbohydrates displayed on the surface of mammalian cells play essential roles in numerous biological processes. In humans, the cell surface is densely decorated with carbohydrates, such as *N*-linked glycans, *O*-linked glycans, and glycans derived from glycolipids [1]. These glycans are composed of a limited set of monosaccharide building blocks, such as glucose (Glc), galactose (Gal), *N*-acetyl glucosamine (GlcNAc), *N*-acetyl galactosamine (GalNAc), fucose (Fuc), and *N*-acetylneuraminic acid (Neu5Ac), yet exhibit immense structural complexity and functional specificity (Fig. 1a). Alteration in glycans is a widely observed feature of cancer and plays a critical role in malignant transformation, metastasis, and immune evasion [2]. Tumor-associated carbohydrate antigens (TACAs) are overexpressed or structurally altered in tumor cells, have emerged as attractive antigens for the development of cancer vaccines [3]. A common strategy involves the chemical synthesis of TACA epitopes and their covalent conjugation to immunogenic carriers to form glycoconjugate vaccines [4]. These glycoconjugates promote antigen uptake by antigen-presenting cells (APCs) through the immunogenicity of carrier proteins, ultimately triggering a carbohydrate-specific adaptive immune response. This includes the $CD4^+$ helper T cell-dependent antibody production pathway and the $CD8^+$ cytotoxic T cell response (Fig. 1b) [5].

Reductive amination between aldehydes and lysine residues on proteins has become a widely adopted strategy for constructing neoglycoproteins which play an essential role in vaccine development and other biopharmaceutical engineering [6–10]. This conjugation method is particularly attractive for its simplicity, mild conditions, and applicability to unmodified proteins. Generally, the carbohydrate substrate bears a free aldehyde moiety either through synthetic derivatization or directly by the reducing end of native oligosaccharides. Under mild aqueous conditions (pH 7.5–8.5, 25–50 °C), the aldehyde reacts with the ε-amino group of lysine to form a Schiff base, which is subsequently reduced to a stable C–N bond using mild reducing agents. This method enables efficient carbohydrate-protein conjugation while preserving the structural integrity of the carrier protein.

In the design of neoglycoprotein-based anticancer vaccines, a key consideration is the ability of APCs to load glycopeptide fragments onto major histocompatibility complex (MHC) molecules for presentation to T cells. For MHC molecules, antigen binding occurs within a peptide-binding groove formed by two α-helixes, while

* Corresponding author.
E-mail address: yongmin.zhang@upmc.fr (Y. Zhang).

https://doi.org/10.1016/j.cclet.2025.112033
1001-8417/© 2026 Published by Elsevier B.V. on behalf of Chinese Chemical Society and Institute of Materia Medica, Chinese Academy of Medical Sciences.

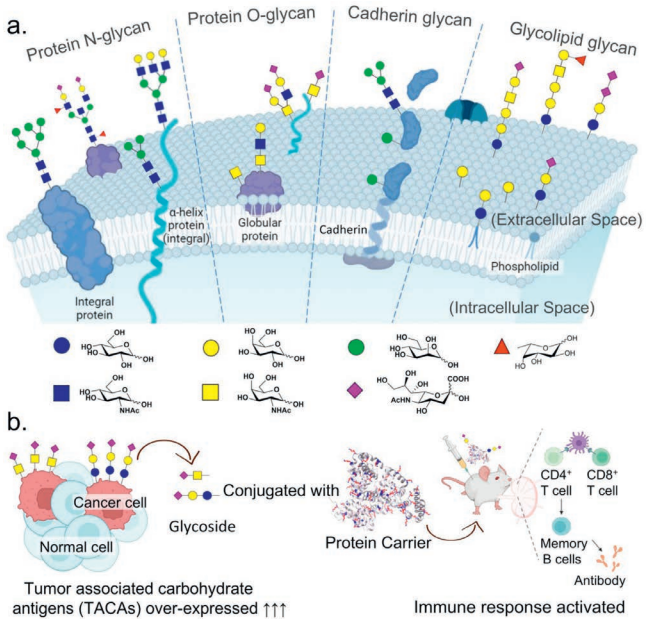


Fig. 1. (a) Mammalian cell surfaces are decorated with abundant and complex oligosaccharides. (b) Certain tumor-associated carbohydrate antigens (TACAs) are overexpressed on cancer cell surfaces and can be loaded onto carrier proteins to activate antitumor immune responses.

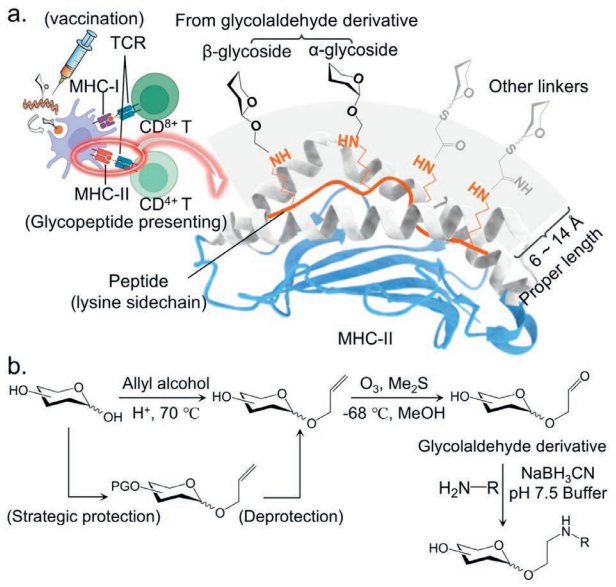


Fig. 2. (a) TACAs conjugated to proteins activate MHC-II-dependent T-cell responses in anticancer vaccines. Degraded glycopeptides are presented to downstream T-cells *via* the MHC-II binding groove. The red bold backbone represents a linear peptide segment with oligosaccharide antigens conjugated to lysine residues flanking outward. Proper linkers should include properties: Short length, flexibility, and the absence of bulky structures. (b) The allyl alcohol glycosylation strategy simplifies the preparation of anchor units. The resulting products, after ozonolysis, can be directly used in aqueous conjugation reactions, ensuring protein activity under physiological conditions.

the glycan portion of a glycopeptide must extend outward at an appropriate angle and distance to be recognized by the T cell receptor (TCR) [11]. Therefore, the spatial presentation of TACAs, including the size of the glycan and the length and flexibility of the linker, is critical for eliciting a specific immune response (Fig. 2a) [12,13]. Rigid or bulky linkers can provoke undesired immune responses to the linker itself and impair TACA recognition, underscoring the need for minimal, non-immunogenic linkers [14]. To this end, allyl groups are often introduced at the anomeric position of the initial monosaccharide to serve as stable, synthetically accessible handles. After oligosaccharide assembly, the terminal alkene is selectively oxidized by ozonolysis to yield the corresponding glycolaldehyde, which can be directly conjugated to lysine-rich proteins *via* reductive amination (Fig. 2b). This allyl-to-aldehyde strategy provides a short, well-defined linker that is chemically stable during synthesis yet positioned within the optimal range for antigen presentation to the immune system, and has been successfully applied in the synthesis of various TACA-based vaccine candidates that elicited promising immune responses in preclinical studies [15–18].

In the course of our recent efforts to develop TACA-based vaccine candidates, we designed a series of non-natural disaccharides by connecting Neu5Ac glycosides to different hydroxyl positions of mannose, glucose, or galactose, and conjugated them to carrier proteins *via* reductive amination. Interestingly, it was observed that different disaccharides exhibited significantly varied loading levels when conjugated to the protein under the same protocol. Notably, despite all substrates bearing aldehyde as the reactive moiety for reductive amination, the α-mannosyl derivative consistently exhibited higher protein loading levels under identical conditions compared to all of other β-glycosidic isomeric counterparts. This preliminary observation motivated us to further investigate the structural factors influencing conjugation efficiency. We initially hypothesized that the anomeric configuration of the glycolaldehyde group on the initial monosaccharide unit might play a key role. To test this, we firstly synthesized a pair of anomeric mannosyl glycolaldehyde derivatives, and used them as substrates for conjugation to bovine serum albumin (BSA), which has 59 lysine residues available for reductive amination. Reactions were carried out at a molar ratio of 5:1 (sugar:lysine residues) in 200 mmol/L phosphate-buffered saline (pH 7.5) at 37 °C, with samples collected every 2 h over a 48-h period. As a preliminary kinetic experiment, each substrate was tested in triplicate to ensure the experimental variability. The α-Man exhibited a faster conjugation rate compared to the β-Man, resulting in an average glycan loading of 54.52 ± 0.34 per BSA molecule after 48 h, whereas the β-anomer reached a lower loading level of 46.87 ± 0.27 under identical conditions, as determined by MALDI-TOF-MS (Fig. 3a).

One of the first factors considered to account for the observed differences in conjugation efficiency was the equilibrium of aldehyde hydration in aqueous buffer. Glycolaldehyde moieties are known to undergo reversible hydration to form geminal diols, potentially reducing the opportunity of free aldehyde available for Schiff base formation. Notably, Bendiak and Fang [19] previously reported that β-glycolaldehyde derivatives can undergo intramolecular cyclization between the C-2 hydroxyl and the hydrated aldehyde (gem–diol) to form a stable 1,4-dioxane-type ring in water (Fig. 3b). We speculated that such cyclic hemiacetals may reduce the effective concentration of reactive aldehyde in solution, thereby lowering the conjugation efficiency. To systematically explore whether this configurational effect is influential, both α- and β-anomeric glycolaldehyde derivatives of four additional monosaccharides were further synthesized for systematically analysis (Fig. 4).

All ten glycolaldehyde substrates were ozonolyzed from their allyl glycoside precursors, which were obtained *via* α-selective Fischer glycosylation or β-selective Koenigs-Knorr glycosylation strategies, followed by purification and ^{1}H NMR characterization (Figs. S1–S10 in Supporting information). In addition to comparing the reactivity differences between α- and β-anomers for each individual glycolaldehyde, we further evaluated the influence of structural features known to affect the formation of cyclic forms in 20 mmol/L phosphate-buffered D_2O (pD 7.5) at a final concentration of 10 mg/mL. The equilibrium distribution of each compound

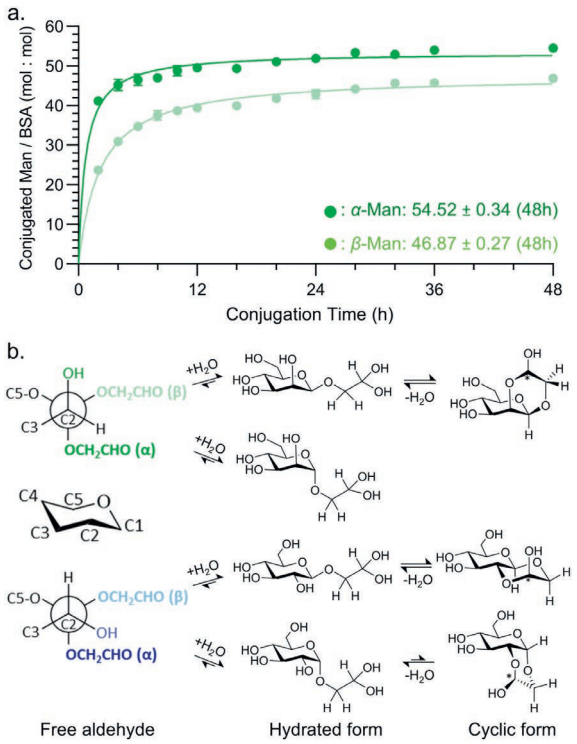


Fig. 3. (a) Reaction track of BSA conjugation with α- and β-mannosyl glycolaldehyde at a molar ratio of 5:1 (sugar:lysine residues) in 200 mmol/L PBS (pH 7.5) at 37 °C. Each number next to the substrate symbol indicates the average number of sugars conjugated per BSA molecule at 48 h. (b) Schematic illustration of the intramolecular cyclization between the hydrated aldehyde form and the C-2 hydroxyl group, as influenced by the stereochemistry of the monosaccharide.

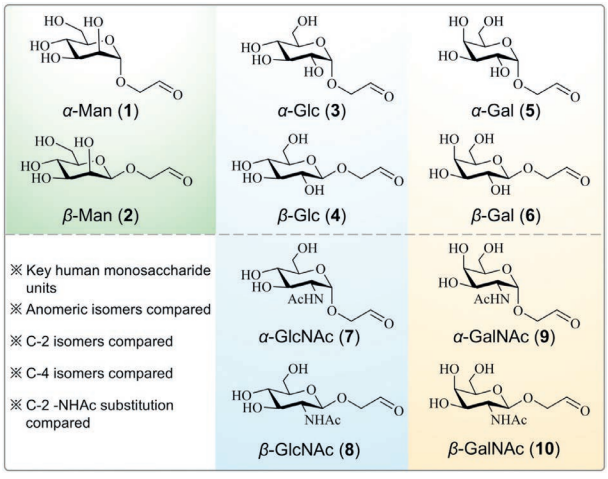


Fig. 4. Ten monosaccharide glycolaldehyde derivatives.

among its hydrated, cyclic, and free aldehyde forms was analyzed by ^{1}H NMR, and the relative abundance of each form was quantified based on the integration of the proton signal on the aldehyde carbon (Figs. S11–S20 in Supporting information). As shown in Table 1, the NMR analysis revealed that the β-Man predominantly exists in a cyclic form (87 %), with the aldehyde signal in the 9–10 ppm region hardly detectable. In contrast, the α-Man exists almost exclusively in the hydrated form (98 %), yet still exhibits a small but distinct aldehyde proton peak at 9.6 ppm, corresponding to approximately 2 % of the free aldehyde. The stable 1,4-dioxane-type ring formed *via* intramolecular cyclization in β-Man effectively suppresses the equilibrium concentration of reactive aldehyde species available for reductive amination, which may account for the lower conjugation efficiency observed for β-Man in Fig. 3a. However, when comparing substrates **3**–**10**, which exhibit varying degrees of cyclization at equilibrium, the relative abundance of free aldehyde species remained consistently around 2 % (β-GalNAc, 3 %), with no significant variation among structures. Subsequently, all ten glycolaldehyde derivatives **1**–**10** were subjected to BSA conjugation under identical conditions to systematically compare their reactivity differences.

Table 1
Equilibrium distribution of glycolaldehyde derivatives.[a]

Substrate	Hydrated form (%)	Cyclic form (%)	Free aldehyde (%)
α-Man (**1**)	98	—	2
β-Man (**2**)	13	87	0
α-Glc (**3**)	84	14	2
β-Glc (**4**)	69	29	2
α-Gal (**5**)	83	15	2
β-Gal (**6**)	66	32	2
α-GlcNAc (**7**)	98	—	2
β-GlcNAc (**8**)	98	—	2
α-GalNAc (**9**)	98	—	2
β-GalNAc (**10**)	97	—	3

[a] Each monosaccharide glycolaldehyde exists in a dynamic equilibrium of hydrated, cyclic, and free aldehyde forms in 20 mmol/L phosphate-buffered D_2O (pD 7.5), as illustrated in Fig. 3b and quantified by ^{1}H NMR integration.

Given the low deviation observed across the three replicates in the preliminary experiment, no parallel reactions were performed in this follow-up study. To accommodate the limited solubility of certain substrates, particularly the β-anomers of Gal and GalNAc, a more diluted buffer was used to ensure complete dissolution and homogeneous reaction conditions for all substrates [20]. As the reduced buffer concentration may slow the coupling reaction, the incubation time was extended to 72 h. Each monosaccharide glycolaldehyde derivative was reacted with BSA at a molar ratio of 5:1 (sugar:lysine residues), corresponding to 15 mg of Hex or 17.5 mg of HexNAc, 15 mg of BSA, and 20 mg of sodium cyanoborohydride ($NaBH_3CN$) in 1 mL of 100 mmol/L PBS buffer (pH 7.5). The results are summarized in Fig. 5, and the corresponding mass spectra labelled with average *m/z* values for each conjugate are listed in Supporting information.

After 72 h of reaction, BSA was conjugated with an average of 49.47 and 38.28 molecules of α-Man and β-Man, respectively. The difference in reaction rates between the two anomers was consistent with the preliminary experiment, while the lower overall conjugation numbers observed here are attributed to the reduced salt concentration of the buffer used in this set of reactions, a factor previously reported to affect the efficiency of reductive amination [10].

For α-Glc and β-Glc, the average conjugation levels were 45.77 and 48.32, respectively, with no significant difference observed between the anomers in either reaction rate or final sugar loading. It was initially hypothesized that the formation of a cyclic 1,4-dioxane intermediate *via* the C-2 hydroxyl and hydrated aldehyde might limit the availability of reactive aldehyde groups, as is possible for α-/β-Glc and α-Man. However, in contrast to this hypothesis, the GlcNAc glycolaldehyde, where the C-2 hydroxyl is replaced by an *N*-acetyl group, exhibited significantly lower reactivity. Despite exhibiting a comparable 2 % free aldehyde signal in the NMR analysis, α-GlcNAc and β-GlcNAc conjugated only 37.92 and 35.73 sugar units, respectively. One possible consideration is that the difference in C-2 substitution between Glc and GlcNAc may lead to more pronounced variations in their molecular polarization characteristics. While both sugars share identical hydroxyl group configurations at the C-3, C-4, and C-6 positions, these sites are known to engage in extensive solvation interactions, including water-bridged

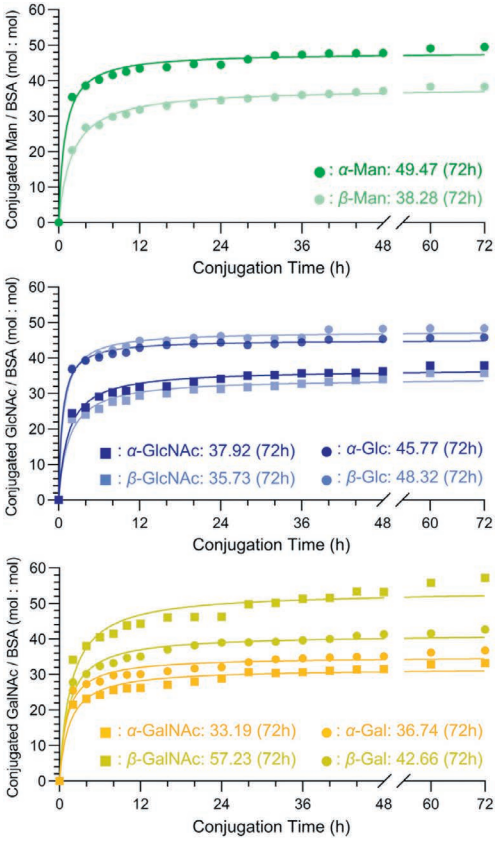


Fig. 5. Reaction track of BSA conjugation with glycolaldehydes at a molar ratio of 5:1 (sugar:lysine residues) in 100 mmol/L PBS (pH 7.5) at 37 °C. Each number next to the substrate symbol indicates the average number of sugars conjugated per BSA at 72 h.

hydrogen bonding networks in aqueous environments [21,22]. In this context, the acetamide at C-2 in GlcNAc may introduce distinct polarization effects, which could influence its behavior and reactivity in the conjugation system.

The α-Gal and β-Gal conjugated to 36.74 and 42.66 sugars per BSA, while α-GalNAc and β-GalNAc conjugated to 33.19 and 57.23 sugars, respectively. In these two pair of comparisons, the β-anomer showed higher reactivity than its α-anomer, especially the comparison between GalNAc. A similar trend between α- and β-anomers of Glc and Gal was previously observed in the formation of Schiff bases with phenylethylamine, as reported in the literature [23]. These observations indicate that aldehyde reactivity is likely governed not only by hydration or cyclization equilibria, but also by the atomic composition and stereo-electronic features of the carbohydrate molecule [24].

To further understand the structural and electronic factors underlying the observed reactivity differences among these glycolaldehyde derivatives, density functional theory (DFT) calculations were performed using Gaussian 09. Geometry optimizations were carried out in water using the B3LYP functional, which combines Hartree-Fock exchange with gradient-corrected correlation from the Lee-Yang-Parr method, providing a reliable balance between accuracy and computational cost for electronic structure analysis. From the energies of the frontier molecular orbitals (FMOs), including the highest occupied (HOMO) and lowest unoccupied molecular orbitals (LUMO), key reactivity descriptors such as chemical potential (μ), chemical hardness (η), global softness (ς), electrophilicity index (ω), and electronegativity (χ) were derived. These parameters offer a quantitative framework to compare the electronic softness, electrophilic character, and potential reactivity trends of each pair of sugar anomers.

According to the FMOs analysis, the LUMO plots of each molecule consistently display electron density localized around the aldehyde carbon (Figs. S23–S27 in Supporting information), which serves as the electrophilic center in the reductive amination process. Lower LUMO values indicate a greater propensity to accept electrons, and thus a higher intrinsic electrophilic reactivity. As summarized in Table 2, comparison between α- and β-anomers for each monosaccharide revealed that the electrophilic reactivity suggested by LUMO energies was generally consistent with the experimentally observed conjugation efficiency. Representative trends include α-Man > β-Man, β-Gal > α-Gal, and β-GalNAc > α-GalNAc, where the anomers with lower LUMO energy values exhibited higher degrees of protein conjugation.

In addition to LUMO energy, two other descriptors, electrophilicity index (ω) and electronegativity (χ), also followed trends that broadly correlated with the experimentally observed reactivity. These three parameters are all conceptually associated with a molecule's capacity to accept electrons during an electrophilic process, making them relevant to the mechanism of Schiff base formation in reductive amination. However, descriptors such as chemical potential (μ), chemical hardness (η), and softness (ς), which relate more to the global electronic stability and polarizability of the molecule rather than site-specific reactivity, did not correlate with the experimental trends. In fact, in most α-/β-anomeric comparisons, the anomer with higher conjugation efficiency paradoxically exhibited a lower chemical potential, greater hardness, and smaller softness. This apparent inconsistency highlights the complex stereo-electronic nature of monosaccharides, particularly in aqueous reaction systems where conformational flexibility, solvation, and transient hydrogen bonding may all influence effective reactivity. While these electronic descriptors appear to offer useful insights into the intrinsic electrophilic character of each molecule, they represent only a simplified approximation of the actual reaction environment and should therefore be interpreted as qualitative indicators rather than definitive predictors of chemical behavior [25,26].

This limitation is further exemplified by the comparison between Glc and GlcNAc anomers. Despite the fact that GlcNAc does not form cyclic intermediates and exhibits a lower LUMO energy (suggesting enhanced electrophilic reactivity), it showed lower conjugation efficiency than Glc. This discrepancy underscores the multifactorial and structurally complex nature of carbohydrates, in which stereochemical configuration, conformational dynamics, and solvation effects act in concert to influence reactivity. As such, it remains challenging to establish a universal rationale for reactivity differences among distinct monosaccharide structures. The present analysis is therefore best suited to rationalizing anomer-specific effects in the context of glycolaldehyde-mediated protein conjugation. While the continuous monitoring experiments reported here clearly demonstrate reactivity variations across different sugar units, this information may serve as a useful reference for selecting the anomeric configuration of the initial unit in neoglycoprotein construction. Nevertheless, a comprehensive explanation for these differences will require future investigations integrating additional structural, thermodynamic, and dynamic parameters.

In conclusion, a series of glycolaldehyde derivatives corresponding to the α- and β-anomers of five common monosaccharides (Man, Glc, Gal, GlcNAc, GalNAc) were synthesized and evaluated for their reactivity toward BSA conjugation *via* reductive amination. These monosaccharides represent typical initial units in the construction of neoglycoproteins for biomedical applications, especially anticancer vaccine development. Conjugation efficiency, monitored over 72 h, revealed clear anomer-dependent trends: α-Man showed higher reactivity than β-Man; α-/β-Glc and α-/β-

Table 2
Associated electronic properties of monosaccharide glycolaldehydes based on DFT modeling.

Electronic Properties	Mannopyranosyl glycolaldehyde		Glucopyranosyl glycolaldehyde		Galactopyranosyl glycolaldehyde		*N*-Acetyl glucosaminopyranosyl glycolaldehyde		*N*-Acetyl galactosaminopyranosyl glycolaldehyde	
	α-Man (**1**)	β-Man (**2**)	α-Glc (**3**)	β-Glc (**4**)	α-Gal (**5**)	β-Gal (**6**)	α-GlcNAc (**7**)	β-GlcNAc (**8**)	α-GalNAc (**9**)	β-GalNAc (**10**)
HOMO (eV) [a]	−7.132	−7.075	−7.024	−7.191	−7.047	−7.126	−6.927	−6.814	−6.861	−6.972
LUMO (eV) [b]	**−0.839** [c]	−0.822	−0.841	**−0.990**	−0.789	**−0.979**	**−1.031**	−0.998	−1.142	**−1.172**
ΔE (eV) [d]	6.293	**6.253**	**6.183**	6.201	6.258	**6.147**	5.896	**5.816**	**5.719**	5.800
μ (eV) [e]	−3.986	**−3.949**	**−3.933**	−4.091	**−3.918**	−4.053	−3.979	**−3.906**	**−4.002**	−4.072
η (eV) [f]	3.147	**3.127**	**3.092**	3.101	3.129	**3.074**	2.948	**2.908**	**2.860**	2.900
Σ [g]	0.159	0.160	0.162	0.161	0.160	0.163	0.170	0.172	0.175	0.172
ω (eV) [h]	**2.524**	2.493	2.501	**2.698**	2.453	**2.672**	**2.685**	2.623	2.800	**2.859**
χ (eV)[i]	**3.986**	3.949	3.933	**4.091**	3.918	**4.053**	**3.979**	3.906	4.002	**4.072**

[a] HOMO: Highest occupied molecular orbital; higher values suggest stronger electron-donating ability.
[b] LUMO: Lowest unoccupied molecular orbital; lower values indicate greater electrophilic reactivity.
[c] Bold values highlight the more reactive anomer (α- or β-) within each pair, theoretically.
[d] ΔE: Energy gap between HOMO and LUMO; smaller gaps generally favor reactivity.
[e] μ: Chemical potential; more negative values indicate lower overall reactivity.
[f] η: Chemical hardness; lower values suggest higher polarizability.
[g] ς: Chemical softness; higher values imply easier electronic deformation and greater reactivity.
[h] ω: Electrophilicity index; higher values reflect stronger tendency to accept electrons.
[i] χ: Electronegativity; higher values indicate stronger attraction for electrons.

GlcNAc exhibited negligible differences between anomers; β-Gal and β-GalNAc outperformed their α-counterparts, typically the β-GalNAc shown the most reactive. These differences are attributed to two factors: The formation of stable cyclic species through condensation between the hydrated aldehyde and equatorial C-2 hydroxyl groups, which reduces the effective concentration of reactive aldehyde, and subtle stereo-electronic differences between anomers. While electronic descriptors alone do not fully predict reactivity across all sugars, they provide mechanistic insight into anomer-specific behavior and offer guidance for the rational selection of monosaccharide configuration in neoglycoprotein design.

Declaration of competing interest

The authors declare that they have no known competing financial interests or personal relationships that could have appeared to influence the work reported in this paper.

CRediT authorship contribution statement

Jiaxu Zhang: Writing – original draft, Methodology, Funding acquisition, Formal analysis, Data curation, Conceptualization. **Xianran He:** Writing – review & editing, Formal analysis. **Gilles Clodic:** Investigation. **Leyu Tang:** Investigation, Data curation. **Jinge Cao:** Investigation. **Yupeng Fu:** Investigation. **Matthieu Sollogoub:** Resources. **Yongmin Zhang:** Writing – review & editing, Supervision, Project administration, Funding acquisition.

Acknowledgments

We thank the China Scholarship Council (CSC) for the Ph.D. fellowship (No. 202108620047 to J. Zhang). Financial supports from the Centre National de la Recherche Scientifique (CNRS) and the Sorbonne Université in France are gratefully acknowledged.

Supplementary materials

Supplementary material associated with this article can be found, in the online version, at doi:10.1016/j.cclet.2025.112033.

References

[1] S. Albrecht, S. Vainauskas, H. Stöckmann, C. McManus, C.H. Taron, P.M. Rudd, Anal. Chem. 88 (2016) 4795–4802.
[2] A. Peixoto, A. Miranda, L.L. Santos, J.A. Ferreira, J. Exp. Clin. Canc. Res. 41 (2022) 143.
[3] C. Sorieul, F. Papi, F. Carboni, et al., Pharmacol. Therapeut. 235 (2022) 108158.
[4] S.S. Shivatare, V.S. Shivatare, C.H. Wong, Chem. Rev. 122 (2022) 15603–15671.
[5] J. Zhang, M. Terreni, F. Liu, M. Sollogoub, Y. Zhang, Biomed. Pharmacother. 176 (2024) 116824.
[6] C. Song, X. Zheng, H. Guo, et al., Glycoconjugate J. 36 (2019) 399–408.
[7] C. Song, S. Sun, C. Huo, et al., Bioorgan. Med. Chem. 24 (2016) 915–920.
[8] Y. Pan, P. Chefalo, N. Nagy, C. Harding, Z. Guo, J. Med. Chem. 48 (2005) 875–883.
[9] Q. Wang, S.A. Ekanayaka, J. Wu, J. Zhang, Z. Guo, Bioconjugate Chem. 19 (2008) 2060–2067.
[10] J.C. Gildersleeve, O. Oyelaran, J.T. Simpson, B. Allred, Bioconjugate Chem. 19 (2008) 1485–1490.
[11] S.A. Malaker, M.J. Ferracane, F.R. Depontieu, et al., J. Proteome. Res. 16 (2017) 228–237.
[12] J.A. Speir, U.M. Abdel-Motal, M. Jondal, I.A. Wilson, Immunity 10 (1999) 51–61.
[13] L.P. Deimel, X. Xue, A. Khan, et al., bioRxiv (2023), doi:10.1101/2023.11.02.565155.
[14] T. Buskas, Y. Li, G.J. Boons, Chem. Eur. J. 10 (2004) 3517–3524.
[15] S. Sun, X. Zheng, C. Huo, et al., ChemMedChem 11 (2016) 1090–1096.
[16] X. Wu, H. McFall-Boegeman, Z. Rashidijahanabad, et al., Org. Biomol. Chem. 19 (2021) 2448–2455.
[17] X. Zheng, F. Yang, M. Zheng, et al., Org. Biomol. Chem. 13 (2015) 6399–6406.
[18] C. Song, X. Zheng, C. Liu, Y. Zhou, X. Ye, Oncotarget 8 (2017) 47330–47343.
[19] T.T. Fang, B. Bendiak, J. Am. Chem. Soc. 129 (2007) 9721–9736.
[20] L. Jäntschi, App. Water Sci. 9 (2019) 1–11.
[21] Y. Zhong, B.A. Bauer, S. Patel, J. Comput. Chem. 32 (2011) 3339–3353.
[22] M. Mohan, V.V. Goud, T. Banerjee, Fluid. Phase Equilib. 395 (2015) 33–43.
[23] J.J. Reina, A. Rioboo, J. Montenegro, Synthesis 50 (2018) 831–845.
[24] J.L. Dashnau, K.A. Sharp, J.M. Vanderkooi, J. Phys. Chem. B. 109 (2005) 24152–24159.
[25] K. Adjir, M. Sekkal-Rahal, M. Springborg, J. Biomol. Struct. Dyn. 41 (2023) 5981–5989.
[26] B.L. Foley, M.B. Tessier, R.J. Woods, Wires. Comput. Mol. Sci. 2 (2012) 652–697.